

# Drought-Tolerant Barley Cultivars: Canopy Temperature as a Phenotyping Tool to Determine Root System Architecture

*A research report submitted to HAN University of Applied Science in partial fulfillment of the requirements for the Bachelor of Science degree in Life Sciences*

Lotus Meijer  
1630801

The University of Queensland  
Queensland Alliance of Agriculture and Food Innovation

Supervisor:  
Prof. Lee Hickey

Date of submission: December 8, 2023

## Abstract

Drought, caused by climate change, poses a significant threat to the production of barley. To ensure high yields, drought adaptation in barley is critical. Roots are primarily responsible for water uptake, and during drought, when water levels are low, deep rooting traits are crucial for developing drought-tolerant crops. However, roots are difficult to study due to their location and therefore a different phenotyping technique using above-ground traits is essential to determine the root system architecture (RSA) of barley during drought. In this study, the relationship between canopy temperature (CT) and rooting depth is explored through thermography. A controlled lysimeter experiment with four genotypes under both drought and well-watered conditions, as well as the results of a large-scale rainfed field trial with 20 genotypes, were used to grow and measure the CT of barley across drought, well-watered, and wet environments. The lysimeter experiment revealed significant differences in CT between climatic treatments ( $P < .001$ ), with barley cultivars under drought experiencing warmer canopies. Additionally, some significant differences in CT were also observed between genotypes ( $P < .05$ ). Barley cultivars with shallow root systems displayed cooler canopies in wet field conditions. Well-watered CT traits were positively correlated with the wet CT traits of the field trial while drought CT traits were negatively correlated with the field CT. Although deeper rooting systems and cooler canopies during drought were suggested by a decrease in CT and an increase in stomatal conductance around flowering time, further research and analyses of the root samples grown under drought conditions are essential to confirm these results. In this study, CT has proven to be a reliable and high-throughput method for breeders to screen root traits and develop future drought-tolerant barley cultivars.

## Table of Contents

Abstract.....	1
List of abbreviations.....	3
Introduction.....	4
Understanding the Potential of Barley Roots in Drought Resistance.....	4
Exploring Above-Ground Traits as Indicators of Root Architecture.....	5
Lysimeters as the Blueprint for Environmental Analysis.....	7
Materials and Methods.....	7
Field Trial Design and Implementation.....	7
Field trial: Canopy Temperature using UAV Sensor Technology.....	9
Field trial: Root Sampling.....	10
Experimental Setup of the RPAD Lysimeter.....	11
Lysimeter Data Collection.....	13
Statistical Analysis.....	14
Results.....	15
Canopy Temperature Variability.....	15
Barley Root Distribution under Wet Field Conditions.....	18
Relationships between Canopy Temperature and Rooting Depth.....	19
Changes in Other Above-Ground Traits.....	20
Discussion.....	21
Conclusion.....	22
References.....	24
Appendices.....	29
Supplementary figures.....	29
Supplementary tables.....	29
Supplementary documents.....	32

## List of abbreviations

ABA	Abscisic acid
BG	Breeding line genotype
BLUPs	Best linear unbiased predictors
BLUEs	Best linear unbiased estimators
CT	Canopy temperature
GS	Growth stage
GSG	Great soil group
$g_{sw}$	Stomatal conductance of water vapour
HDM	Hierarchical data model
IR	Infrared
LSD	Least significant difference
NR	Non-reproductive
OSAVI	Optimised soil adjusted vegetation index
PCA	Principal component analysis
PC	Principal component
QAAFI	Queensland Alliance for Agriculture and Food Innovation
RPAD	root zone, plant-atmosphere, drainage
RSA	Root system architecture
SpATS	spatial analysis of field trials with splines
TC	Tiller count
UAV	Unmanned aerial vehicle
WHC	Water holding capacity

## Introduction

Barley (*Hordeum vulgare* L.), is one of the major cereal crops globally. It is widely used in the brewing industry as well as a source of food and feed for livestock. To keep up with the ever-growing demand for barley, it has become the fourth most-produced cereal crop in the world (FAO, n.d.). Although barley is adaptable to various climates, prolonged drought stress negatively impacts grain yield (Nezar H. S., 2005; Högy et al., 2013). Climate change is associated with widespread changes in weather patterns, causing increasingly extreme weather events such as heavy precipitation, heat waves and drought (IPCC, 2023). This climate variability is detrimental to the production of barley and causes threats to food security and livelihood (Brown et al., 2019; IPCC, 2023). The effects of prolonged drought were evident in the 2019-20 growing season in Australia as bulk grain production fell over 30% nationwide, with some states seeing reductions up to 66%, resulting in Australia's lowest grain production since 2007-08 (Brown et al., 2019; Australian Competition and Consumer Commission [ACCC], 2021). With El Niño on the doorstep and predictions revealing dry anomalies and record-breaking temperatures for the 2023-2027 season, crop adaptation and changes to agronomic practices for barley cultivation are required to breed for drought adaptation traits and consequently ensure high yields (World Meteorological Organization [WMO], 2023; Dijkman et al., 2017). Drought adaptation is complex, involving many different component traits that regulate physiological, morphological, and cellular processes such as root architecture, leaf area, canopy temperature, stomatal conductance, photosynthetic rate and hormonal production (Basu et al., 2016; Mahmood et al., 2019; Zia et al., 2021; Pradhan et al., 2022). The interactions between these traits are complex, species-specific, and vary based on environmental conditions. For cereal crops, these interactions are not yet fully understood. This study will particularly focus on root traits and canopy temperature to investigate their role in drought adaptation.

### *Understanding the Potential of Barley Roots in Drought Resistance*

Alterations in water availability due to climate variability are key factors to consider when selecting root traits in barley. Resource acquisition is one of the main functions of roots however different climate conditions call for different root distributions depending on the availability of water in the ground. While the importance of roots and the need for differences in root system architecture (RSA) is known, the effect of climate variability on barley roots remains understudied.

It has been demonstrated that deeper rooting is crucial for accessing deep water sources, making it a requirement for crops in drought-prone environments. However, methodological challenges have hindered the exploitation of root traits, particularly those in field-grown plants (Wasson et al., 2014). Traditional root phenotyping techniques, such as trenching, shovelomics or soil coring are laborious, time-consuming and have many limitations (Topp et al., 2016; McGrail et al., 2020). Trenching involves excavating the site with heavy machinery to create thin trenches from which the roots can then be manually excavated and imaged (Weaver et al., 1922). While trenching provides comprehensive and accurate knowledge about the root system in real-life conditions, it requires a great amount of time to obtain the trenches and fill these again before harvest. Shovelomics has been used to phenotype crown roots. As this method only requires the upper layer of the roots to be excavated to study the crown roots, it is a significantly faster method (Trachsel et al., 2011). However, only partial RSA can be determined, and the roots can only be studied once, at one stage (Takahashi & Pradal, 2021). The coring technique provides cores of up to 2m deep, to estimate the root distribution in the entire soil profile. While the cores are obtained rapidly, this method offers limited root data. It is difficult to determine the RSA accurately and the root structure may be misrepresented due to missing root pieces or inclusions of neighbouring plants. In addition to being

time-consuming and laborious with often a high root data loss rate, these methods are also destructive to the field and the plant, resulting in yield loss (McGrail et al., 2020; Li et al., 2022).

Rhizoboxes and other glasshouse-based growth containers offer the option to phenotype roots rapidly in comparison to field-based experiments. For example, Rhizoboxes contain translucent walls to observe root growth throughout the plants' developmental stages in a non-destructive way and perform measurements on the root system using high-quality imaging. However, the Rhizoboxes need to be very thin to visualise the roots on the walls, resulting in reduced growing space for the roots. Roots grown in Rhizoboxes or other glasshouse containers, do therefore not represent root growth in field conditions (Lesmes-Vesga, 2022). Lysimeters provide much more growing space than most other glasshouse containers, however just like in the field, the roots are hidden under soil. Lysimeter and glasshouse-based experiments provide controlled climatic environments and allow root samples of individual plants to be studied efficiently without the inclusion of roots from neighbouring plants. However, due to the limited growth space, field-based phenotyping is needed to obtain accurate results and determine the RSA of crops.

Therefore, other high-throughput, non-invasive, and accurate phenotyping methods are needed to measure root traits under realistic large-scale field or breeding conditions. Above-ground traits, such as CT, have the potential to serve as effective screening tools and a proxy for below-ground traits. Not only would above-ground trait-based screening methods meet the criteria for RSA screening mentioned above, but they also offer the additional benefit of being able to be measured repeatedly throughout various growth stages of a single plant.

#### *Exploring Above-Ground Traits as Indicators of Root Architecture*

CT is a direct function of the plants' transpiration and is closely related to stomatal conductance, which regulates the exchange of water vapour and carbon dioxide between the leaves and the environment. A change in CT could indicate a change in stomatal conductance and, therefore, a change in water use efficiency (Rebetzke et al., 2012). To prevent excessive water loss, stomata closure is induced via abscisic acid (ABA) synthesis in the guard cell when there is limited access to water, resulting in an increase in CT (Malcheska et al., 2017). Previous studies on wheat and rice have shown that deeper root systems lead to cooler canopy temperatures under drought conditions (Hirayama et al., 2006; Lopes & Reynolds, 2010; Pinto & Reynolds, 2015; Li et al., 2019). Therefore, it is believed that barley varieties with a deeper root system can access soil water located at deeper levels, leading to more open stomata and active transpiration, resulting in a cooler canopy under drought conditions (Fig. 1).

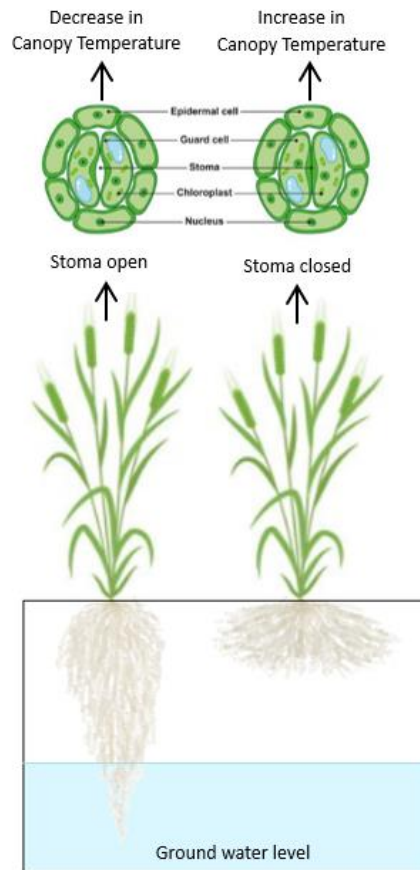


Figure 1: Schematic representation of how different root system architectures (RSA) affect the stomata state and subsequently the canopy temperature during drought in barley.

Various techniques are available for phenotyping CT, which can be divided into two categories: airborne or ground-based. Airborne techniques have been proven to be more suitable for field experiments as they are more cost-effective, more accurate and less time-consuming than ground-based techniques, as shown by Deery et al. (2016) and Li et al. (2019). In both studies, airborne thermography from a manned aircraft using a thermal camera was used to phenotype CT in large-scale field trials. Adopting this technique is costly due to the expenses associated with the aircraft and their maintenance. Additionally, compared to other airborne remote sensing methods like satellites or drones, the use of manned aircrafts poses a higher accident risk (Rejeb et al., 2022). Extensive comparisons and reviews of each remote sensing technique and its application in agriculture have been conducted in the past. A review by Rejeb et al. (2022) summarised a significant amount of literature on remote sensing technologies, revealing that despite their own limitations, using unmanned aerial vehicles (UAVs) is the most suitable technique for phenotyping CT in a field trial. While drones are sensitive to environmental conditions such as rain and wind, have a limited flight duration due to limited battery life and have a limited payload weight, they are more cost-effective, safer and offer higher repeatability than the aircraft technique (Rejeb et al., 2022). Drones can also produce high-quality and high-resolution images on cloudy days, which is not possible using satellites (Manfreda et al., 2018; Rejeb et al., 2022).

Although airborne remote sensing techniques are more advantageous to use than handheld ground-based phenotyping techniques in field experiments due to the latter being time-consuming and sensitive to short-term weather fluctuations, they cannot be used in glasshouse experiments (Deery

et al., 2016). Handheld infrared (IR) thermometers and thermal IR cameras are therefore often used to phenotype CT in glasshouses instead. While both techniques are sensitive to minor changes in weather conditions while measuring and time-consuming, they record CT differently (Deery et al., 2016; Lo et al., 2018). IR thermometer can only detect the temperature of one spot within the canopy, while a thermal camera can record the temperature for the entire canopy, obtaining a more accurate overall temperature. As the thermal IR camera can capture the temperature of all objects within the image to determine the average temperature, it will also include any background temperatures such as soil when the canopy is sparse (Lo et al., 2018). Fortunately, extraneous temperatures can be excluded using software to obtain reliable results (Deery et al., 2016).

### *Lysimeters as the Blueprint for Environmental Analysis*

The main objective of this study is to investigate whether CT can be used as a suitable phenotyping method to characterise barley cultivars for root distribution under drought conditions. Based on the results of previous studies on other cereal crops, it is expected that genotypes that measure cooler canopy temperatures will have deeper root systems under drought conditions (Hirayama et al., 2006; Lopes & Reynolds, 2010; Pinto & Reynolds, 2015; Li et al., 2019). Our research team performed a large-scale field trial in 2022 to phenotype barley roots, however unpredictability of the weather and the inability to control the water supply during the field trial necessitated a second experiment with a controlled environment to implement drought. We used lysimeters to create controlled drought- and optimal conditions and explored environmental and genotypic variation in CT for four genotypes. The results of this study could help breed drought-tolerant barley cultivars by allowing breeders to quickly measure barley's abiotic stress tolerance using CT and subsequently select drought adaptation traits.

## **Materials and Methods**

This study uses a multi-environmental lysimeter experiment to understand the relationship between CT and rooting depth for barley in drought and well-watered conditions. Due to time constraints, the roots of the lysimeter experiment could not be analysed for this report and therefore root data from a previously conducted field experiment is used to correlate and interpret the above-ground data obtained during the lysimeter experiment. In 2022, the research team of the Queensland Alliance for Agriculture and Food Innovation (QAAFI) at the University of Queensland conducted a field trial in which the root distribution of 20 barley genotypes was studied. An unmanned aerial vehicle (UAV) was utilised to capture various above-ground traits, including CT. However, due to the wet climate conditions throughout the field trial, the research team could not determine the root growth of barley in drought conditions and the lysimeter experiment was required to obtain those results.

### *Field Trial Design and Implementation*

The field trial was conducted in the Darwin field at The University of Queensland Gatton Farms, located in the Lockyer Valley Region in Southeast Queensland, Australia (-27.545, 152.354). With Lockyer Creek in close proximity as well as the presence of underground bores, the site has access to irrigation. The soil at this site is classified as a Black Vertosol, which is a soil type consisting of a clay texture with various densities depending on the soil depth and is part of the Great Soil Group (GSG) known as Black Earths (National Committee on Soil and Terrain & Isbell, 2016; Queensland Government, 2023).

The barley seeds were sown on June 16<sup>th</sup>, 2022, and harvested over two days on November 10<sup>th</sup> and 11<sup>th</sup>, 2022. The daily rainfall and temperature data recorded by the on-site weather station located on the Eastern side of the field trial is presented in Fig. 2. The average annual rainfall for this area is 668.6 mm (1991-2020), of which the majority occurs in the warmer summer months (December-February). The average annual maximum and minimum temperatures are 27.6 °C and 13.3 °C (1991-2020) (Bureau of Meteorology, 2023). It is noticeable that there was greater precipitation than usual for this time of year throughout the entire field trial, with a significant peak of rain towards the end of the trial. This resulted in a delay in harvest.

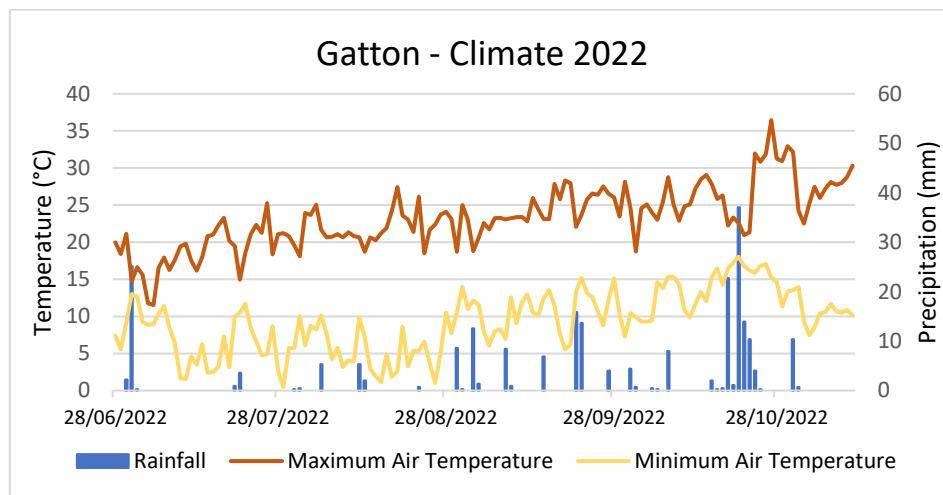


Figure 2: Daily minimum and maximum air temperature, and rainfall recorded at The University of Queensland Gatton Farms, Southeast Queensland, Australia from June 16<sup>th</sup> to November 11<sup>th</sup>, 2022.

The field trial consisted of twenty different barley genotypes that are most representative of the Australian breeding germplasm and part of the InterGrain Pty Ltd breeding program. Twelve of these genotypes are breeding lines while the other eight are commercial: Buff, Compass, Fathom, Maximus CL, RGT Planet, Rosalind, Scope CL, and Spartacus CL. The genotypes were previously phenotyped by InterGrain Pty Ltd and selected based on their similarity in phenology and divergence in root angles. The root angle is determined by the gravitropic response, causing a narrow root angle that is representative of a steep and deep RSA or a wide root angle that is representative of a shallow RSA (Oyanagi, 1994). Each genotype was sown as part of a randomised replicated design with 6.0 replicates. Therefore, 120 plots with a plot size of 2.0x5.0 m were used in this experiment. The plots were arranged across 4 rows, each containing 30 columns with column spacing of 1 m (Fig. 3). Each side of the field trial was surrounded by at least one row of buffer, consisting of wheat. In addition, the experiment was surrounded by other field trials and buffer rows to avoid any possible edge effects.

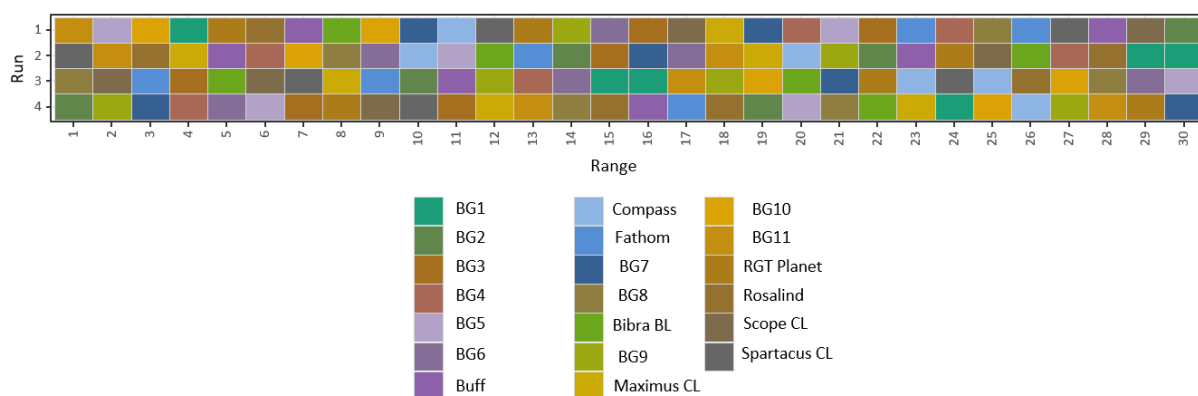


Figure 3: The layout of the 20-genotype barley field trial at The University of Queensland Gatton Farms, Southeast Queensland, Australia in 2022. Each genotype has 6 replicates that are randomly distributed across the 4x30 plots field. Twelve out of the twenty genotypes are breeding lines, labelled breeding genotype (BG) 1-11 as well as Bibra BL. The remaining eight genotypes, Buff, Compass, Fathom, Maximus CL, RGT Planet, Rosalind, Scope CL, and Spartacus CL are commercial lines.

Fertiliser and pest control sprays were applied to the plots on three separate dates during the field trial. On June 17th, a pre-emergent herbicide spray was applied using Boxer Gold (800g/L Prosulfocarb, 120g/L S-Metolachlor) and Glyphosate (540g/L), at a rate of 2.5L/ha. The solution was applied through 200L of water per hectare. On July 20th, granular urea 46% N was used for fertiliser spreading at a rate of 150kg/ha. On July 29th, a selective herbicide spray was applied using Starane Advanced (333g/L Fluroxypyr), at a rate of 600ml/ha. This herbicide was applied through 200L of water per hectare. Additionally, a fungicide spray was also applied using Amistar Xtra (200g/l azoxystrobin, 80g/L cyproconazole), at a rate of 800ml/ha. The fungicide was applied through 100L of water per hectare.

#### *Field trial: Canopy Temperature using UAV Sensor Technology*

The CT was measured on sixteen dates with the first flight when the Barley was at the mid-late tillering stage and the last flight at physiological maturity. The growth stage (GS) according to Zadoks was only scored for Maximus and RGT Planet throughout the field trial (Zadoks et al., 1974; Department of Primary Industries and Regional Development [DPIRD], 2018). The CT was measured on the following dates: 27<sup>th</sup> of June; 15<sup>th</sup>, 18<sup>th</sup>, and 28<sup>th</sup> of July; 2<sup>nd</sup>, 9<sup>th</sup>, 16<sup>th</sup> and 23<sup>rd</sup> of August; 5<sup>th</sup>, 12<sup>th</sup>, 21<sup>st</sup> and 30<sup>th</sup> of September; 4<sup>th</sup>, 11<sup>th</sup>, 26<sup>th</sup>, 31<sup>st</sup> of October. On each day, the flight commenced around 10:00 AM and took approximately 20 minutes upon completion. The CT was measured using a Matrice 300-RTK drone (SZ DJI Technology Co., Ltd., Shenzhen, Guangdong, China) equipped with a multispectral camera sensor namely MicaSense Altum (AgEagle Aerial Systems Inc., Seattle, WA, USA). The flight trajectory for the UAV was programmed prior to the first flight using the remote controller and was set to an altitude of 20m above ground. This automated flight path was followed during each flight. The MicaSense Altum is a thermal camera that has a shutter speed of 1/800 seconds and produces images with 80% overlap and high resolution of ~1 cm<sup>2</sup> pixel. The camera was calibrated prior to and post each flight by holding the drone with the Altum sensor camera 1 meter above an automated calibration panel with 50% reflectance of each light band. This allows for radiometric calibration, which is necessary to account for the changes in light conditions between the start and finish of the flight mission.

The CT data for each plot were extracted from the orthomosaic images generated using Agisoft Metashape 1.7.3 (Agisoft LLC, 2021). Several steps were followed to develop these orthomosaic

images including, 1) image alignment 2) calibration and optimisation using 12 Ground Control Points (GCPs) with known coordinates 3) development of georeferenced dense point cloud and digital elevation model and finally 4) generation of orthomosaic image that has 5 rasters for each of the light bands and thermal. ArcMap within the ArcGIS software 10.8 (Esri, 2020) is used to create a shape file of the field trial that assigns each plot ID to its respective coordinate in the field. Lastly, the inhouse package developed by researchers at the University of Queensland 'Xtractor' was used in a Python environment (Python Software Foundation, <https://www.python.org/>) to extract CT datasets and several vegetation indices such as the optimized soil-adjusted vegetation index (OSAVI). Using OSAVI masking, the real temperature of the vegetation is calculated by excluding background temperatures from e.g., the soil. Detailed information on the extraction process in Xtractor is reported in Das et al. (2022). Fig. 4 provides an orthomosaic of the field trial using the mean CT with an OSAVI mask applied, for the UAV flight of August 23, 2022.

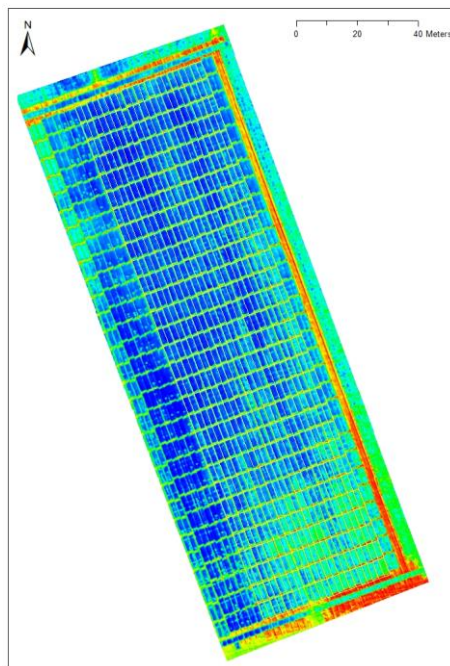


Figure 4: A thermal orthomosaic with OSAVI mask application of the Darwin field at The University of Queensland Gatton Farms, Lockyer Valley Region, Southeast Queensland, Australia. Generated using the UAV flight thermal images of the 20-barley genotype field trial on August 23, 2022.

#### *Field trial: Root Sampling*

The soil coring technique was used on the 20-genotype barley experiment to phenotype the roots. Root coring was carried out for two weeks during the flowering period (September 19th to 30th). The aim was to collect four cores from each plot, two on the plant rows and two between them, from a total of 120 plots. Unfortunately, due to extremely wet soil, it was not possible to collect cores from some of the distant plots. The collected cores were utilized to measure roots by counting the root numbers using the core-break approach (Wasson et al., 2014). Additionally, a subset of the cores was washed to scan the roots and measure their dry weight.

To obtain soil samples, a 2 m stainless-steel soil corer mounted on a tractor was utilized to extract sampling cores from the ground. The cores were emptied into a cradle and manually broken into 10 cm segments, spanning from 10-180cm in depth. As per the core-break method, the exposed live

roots on either side of each core are counted and combined for each depth. The implementation of the core breaking technique has proven to be a more time-efficient method compared to the traditional root-washing approach (Wasson et al., 2014).

#### *Experimental Setup of the RPAD Lysimeter*

Following the initial field trial, a similar experiment was performed however on a much smaller scale and with controlled environments. Specialised machinery named lysimeters were used during the second experiment. The RPAD (root zone, plant-atmosphere, and drainage) lysimeter system is an automated system that can control the supply of water at three levels and measure water use through periodic weighing. With this system, it was possible to create both drought and well-watered treatments for each genotype involved, allowing root development to be observed under various climate conditions. Offering a controlled environment, the research conducted in the lysimeter is advantageous as the effects of climate change are evident in the increased variability of weather patterns, which poses significant challenges to the management of field trials. With the unpredictability of weather conditions, it becomes difficult to control and regulate the climate in a manner that is conducive to the success of such trials (Mohan et al., 2023).

Four barley genotypes were selected from the twenty previously tested during the field trial. Three of these genotypes are commercial lines, namely Maximus CL, Spartacus CL and RGT Planet while the fourth genotype is a breeding line from InterGrain. Throughout this report, this genotype will be referred to as Bibra BL. The selection of four genotypes was made based on the similarity of certain traits, albeit with contrasting root distributions. The uniformity in flowering time observed across all four genotypes enables accurate comparisons, given that flowering time serves as a key indicator for the developmental timeline for other above- and below-ground traits. Additionally, flowering time is a major factor in environmental-based crop adaptation (Nakamichi, 2014; Trevaskis, 2018).

The barley was sown in the RPAD lysimeters on the 6<sup>th</sup> of July 2023 and harvested while 90% of the productive vegetation was in the flowering stage on the 25<sup>th</sup> of September (Zadoks et al., 1974; DPIRD, 2018). The drought treatment was implemented on the 7<sup>th</sup> of August once the majority of plants reached the mid-tillering growth stage by reducing the water holding capacity (WHC) to 50%. The well-watered treatment was characterised by a WHC of 80%, creating an optimal environment. The selection of the well-watered and water-deficit targets was based on the WHC ranges that have been applied previously in the published literature on water deficit treatments in barley (Hellal et al., 2019; Islam et al., 2022).

The experiment was designed with eight lysimeter tables, each containing eight soil cores. This resulted in a total of 64 cores to be included in our experiment (Fig. 5). In Appendix A, a schematic drawing of a single RPAD table with its corresponding dimensions is displayed. Each table is connected to a secondary computer that communicates with the primary controller. The primary controller can schedule adjustments to the water supply at each level of every core. During this experiment, water is only supplied at level 2 to prevent water logging but mimic drought conditions in the field. The weight of each core is recorded at 30-minute intervals, and this data is accessible via an online server for remote water supply adjustments and error detection. Each cylindrical core has a diameter of 1000x300 mm and comprises six soil bags, each with a volume of approximately 1 L. The soil bags are arranged in two per level, allowing for the capture and analysis of roots upon harvesting (see Appendix A). Heavy clay, a similar soil type to the one used in the field trial, was used during this experiment.



Figure 5: Overview of the RPAD experiment including 64 samples, consisting of four different barley genotypes: Maximus CL, RGT Planet, Bibra BL, and Spartacus CL. Each genotype is represented by eight well-watered and eight drought-treated replicates.

The experiment took place in the Lysimeter Facility at the University of Queensland Gatton Campus. This facility consists of a glasshouse and a workshop. A weather station located in the southeast corner of the glasshouse recorded the internal temperature every 15 minutes. This weather station was synchronised to the secondary computer of each of the eight lysimeter tables. The daily mean light hours and mean dark hours temperatures recorded within the glasshouse during this experiment are displayed in Fig. 6. Light hours represent the time between sunrise and sunset and are calculated using the Geodetic Calculator for Gatton 2023 AEST (27° 33' S, 152° 16' E) (Geoscience Australia, n.d.).

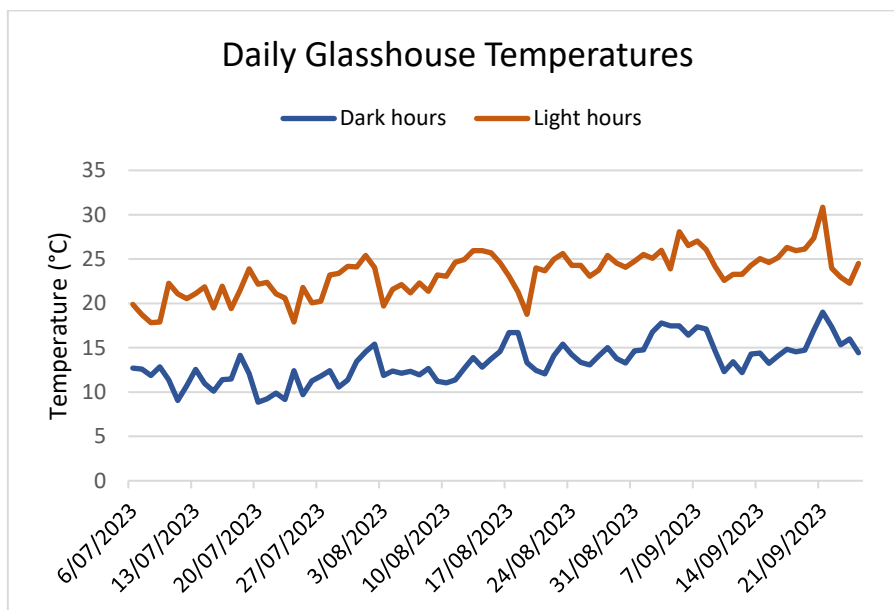


Figure 6: Daily mean temperatures for the light and dark hours, Gatton, Southeast Queensland, Australia, from July 6<sup>th</sup> to September 25<sup>th</sup>, 2023.

In order to decrease the amount of evaporation, a layer of 3mm polypropylene beads is placed on the topsoil in each soil core. This creates a protective barrier against moisture loss and limits direct contact of the soil with the air and sunlight. As a result, the absorption of water by the barley roots can be observed with greater reliability. Furthermore, the use of polypropylene beads helps to minimise variability and enhance the repeatability of the experiment.

Upon soil analysis, fertiliser was mixed in with the soil prior to filling the lysimeter cores. 100 g N (urea), 120 g K (Muriate of potash), 40 g S ( $\text{CaSO}_4 \cdot 2\text{H}_2\text{O}$ ) and 4 g Zn ( $\text{ZnSO}_4 \cdot 7\text{H}_2\text{O}$ ) were added per 800 kg of soil. No further fertiliser was added throughout the experiment. The crop was sprayed three times for mildew and aphids. To prevent skin irritation, gloves and long-sleeved clothing were worn when handling the plants within a 72-hour window after the treatments.

### *Lysimeter Data Collection*

During the RPAD lysimeter experiment, the CT was recorded weekly from mid-tillering until flowering using the FLIR T420 Thermal Imaging Infrared Camera (Teledyne FLIR LLC, Wilsonville, OR, USA). The camera was set to a 0.95 emissivity, 21°C reflected temperature, iron bow colour palette, and the closest object distance setting of 1m. The camera was positioned on a tripod and orientated laterally towards the barley crop, capturing the top 20 cm of the crop from a distance of approximately 25 cm. The CT was measured every seven days between 10:00 AM and 12:00 PM, following the same order. To ensure consistency in the measurements, 5 mm corflute boards were utilised to create a uniform background and the camera was calibrated prior to each measurement using melting ice (Teledyne FLIR, n.d.). The CT was measured on the following seven dates: 8<sup>th</sup>, 15<sup>th</sup>, 22<sup>nd</sup> and 29<sup>th</sup> of August; 5<sup>th</sup>, 12<sup>th</sup> and 19<sup>th</sup> of September. Three images per core per time point are imported into the software ResearcherIR 4.40.12 (Teledyne FLIR LLC, Wilsonville, OR, USA) to remove the background temperature using the interval isotherm function, to find the corrected average CT per core before further statistical analysis.

Throughout the experiment, a range of other above-ground characteristics were measured including tiller count (TC) and stomatal conductance to water vapour ( $g_{sw}$ ). These measurements were recorded twice a week, at the start and the end of the week. The tiller count was closely monitored from the early tillering stage (GS 21) until flag leaf emergence (GS 37) throughout the experiment. A final tiller count took place upon harvest. An LI-600 porometer (LI-COR Inc., Lincoln, NE, USA) was used to collect the  $g_{sw}$ , taking measurements consistently at 10 AM and in the same order from the early seedling growth stage until harvest. A final tiller count was performed upon harvest. The LI-600 porometer calculates  $g_{sw}$  by creating a confined space under the leaf blade using a humidity sensor. The leaf area created by this particular porometer is 0.44 cm<sup>2</sup>. Within this leaf area ( $s$ ), the porometer measures water vapour before ( $W_{ref}$ ) and after ( $W_{sam}$ ) interaction with the leaf surface. Using these measurements and the flow rate ( $\mu$ ), transpiration ( $E$ ) can be calculated:  $E = \frac{\mu(W_{sam} - W_{ref})}{s}$ . The instrument can then determine the total conductance to water vapour ( $g_{tw}$ ) and boundary layer conductance, eventually calculating  $g_{sw}$  (LI-COR, 2023). The  $g_{sw}$  measurements taken on the 12<sup>th</sup> of September 2023 are excluded from analyses, due to incorrect measurements by human error. Furthermore, data for sample 7.2 is excluded from all data analysis including CT from August 31, 2023, due to a defect in the water supply to this core. In addition to the porometer measurements, each core was scored for Zadoks' GS (Zadoks et al., 1974; DPIRD, 2018).

### *Statistical Analysis*

The (pre-processed) data from the 2022 field trial and the 2023 lysimeter experiment are statistically analysed and visualised using RStudio 2023.6.1.524 (Posit team, 2023), a statistical computing software that utilizes the R 4.3.1 programming language (R Core Team, 2021).

Above-ground traits such as TC,  $g_{sw}$ , CT measured in the field and CT measured in the lysimeter, were spatially corrected at various time points. A linear mixed model by residual maximum likelihood using the software 'ASReml-R' (version 4.2.0), is utilised to fit the data for each timepoint and eliminate spatial variation across each experiment (Butler et al., 2023). The fixed effect is tested for linear run and linear range, while the random effect is tested for replicates, run and range. Additionally, treatment is accounted for with a fixed effect where applicable, while genotype is accounted for with a random effect. Lastly, the model includes autoregression residuals for both column and row to allow for autocorrelation of the two-dimensional data. The significance ( $P < 0.05$ ) for each fixed parameter in the fitted model is determined by means of the Wald test with the function `Wald` (Butler et al., 2023). The loglikelihood ratio is used to determine the significance ( $P < 0.05$ ) of random effects. Furthermore, broad-sense heritability ( $H^2$ ) is calculated to evaluate the quality and the repeatability of the data. Finally, the Best Linear Unbiased Predictors (BLUPs) and Best Linear Unbiased Estimators (BLUEs) are calculated for each time point in both experiments.

Differences within genotypes and treatments across genotypes were tested for significance by means of pairwise comparison using Fisher's Least Significant Differences (LSD) with a default level of alpha 0.05. The p-value for each comparison is calculated using the BLUEs with the function `predictPLUS` from the R package 'asremlPlus' (Brien, 2023).

The root count analysis involved a two-stage process: Firstly, a linear mixed model was used to account for operator and spatial effects. The root count for each genotype of the 2022 field trial was adjusted by means of a SpATS model (Spatial Analysis of Field Trials with Splines) using the R package 'mgcv'. Secondly, a Hierarchical Data Model (HDM) was used to model the genotypic signal and describe the root distribution of these root traits over soil depths. The R scripts "Help functions Pspline Hierarchical Curve Data Model" and "Functions Pspline Hierarchical Curve Data Model" (Pérez-Valencia et al., 2022), and the R packages 'splines', 'spam' and 'statgenHTP' were used for this. The R package 'ggplot2' was used for data visualization throughout all statistical analyses in this report (Wickham, 2016). Best linear unbiased predictions (BLUPs) are calculated at each depth using the chosen model in which the effect of operator and genotype was accounted for with a random effect. Finally, the root depths are combined into four layers based on the local soil profile and BLUPs are calculated per layer using 'ASReml-R' based on the previously found final model. (Table 1).

Table 1: The Black Vertosol soil profile morphology at the Darwin field (-27.545, 152.354) in The University of Queensland Gatton Farms, Lockyer Valley Region, SE Queensland, Australia (National Committee on Soil and Terrain & Isbell, 2016; Queensland Government, 2023).

Soil layer number	Soil layer name	Upper depth (cm)	Lower depth (cm)	Soil Colour	Soil Texture
1	Ap	0	20	Dark grey	Light-medium clay
2	B21	20	65	Dark red/brown	Medium clay
3	B22	65	90	Dark red/brown	Medium clay
4	D1	90	150	Dark red/brown	Silty clay

Phenotypic correlations were explored between selected CT of specific barley growth stages across the field trial and the lysimeter experiment, by means of principal component analysis (PCA) using the `prcomp` function. Upon further selection of CT data points, a second PCA was performed for rooting depth and CT. The correlations are presented in biplots that show the two largest principal components (PC), with the contribution to the overall variance indicated for each variable, using the ‘factoextra’ package in R (Kassambara & Mundt, 2020).

## Results

### *Canopy Temperature Variability*

Spatial analysis indicated great spatial variation of canopy temperature (CT) in the lysimeter and revealed potential outliers (Table 2, Supplementary Figure S1). Upon eliminating the spatial discrepancies of the design, highly significant treatment effects ( $P < .001$ ) were observed throughout the last five subsequent growth stages (Table 2). The high heritability of the majority of the measurements suggests that the variability in CT is predominantly attributed to genetic differences with negligible contribution from environmental factors (Table 2).

Table 2: Linear mixed model results for canopy temperature (CT) on seven dates, incorporating fixed effects of treatment, linear column and linear row. ‘NA’ indicates not applicable. Heritability ( $H^2$ ) for CT is calculated for each date.

	Treatment	Linear column	Linear row	$H^2$
08-08-2023 GS26	0.207	NA	NA	-0.000
15-08-2023 GS29	0.074	0.021	NA	0.819
22-08-2023 GS31	0.000	NA	NA	0.971

29-08-2023 GS32	0.000	NA	0.047	0.993
05-09-2023 GS36	0.000	0.011	0.010	0.984
12-09-2023 GS47	0.000	NA	NA	0.959
19-09-2023 GS53	0.000	0.003	NA	0.970

As seen in Fig. 7, the smallest differences in CT for the four genotypes between the two climatic conditions were observed on August 8th, prior to the onset of the drought treatment, suggesting that all 64 barley samples were comparable. The CT variation peaked on August 29th and September 5th during the mid-to-late stem elongation stage of barley cultivars, with high CT recorded for the ones experiencing drought stress. This increase in variation is also observed by heightened significant differences in treatment effect and heritability for both dates (Table 2). In Fig. 7, a sharp decline in temperature is observed during the later growth stages, indicating potential adaptations taking place in response to drought stress (Nakamichi, 2014; Trevaskis, 2018).

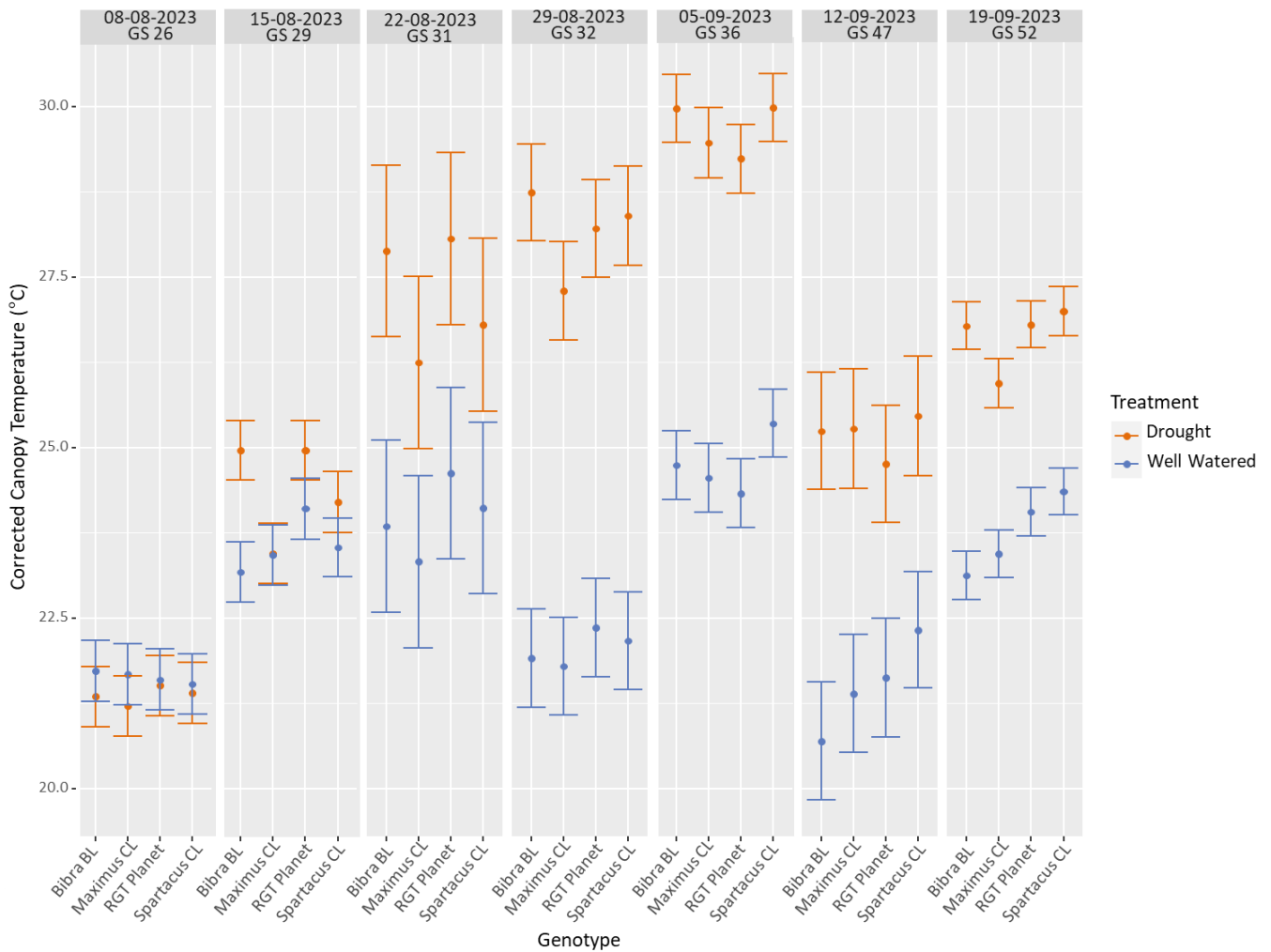


Figure 7: Spatially corrected canopy temperatures (CT) for barley genotypes Bibra BL, Maximus CL, RGT Planet and Spartacus under drought- and well-watered treatments, presented for each date/growth stage. Error bars reflect standard error.

A pairwise comparison provided a clear insight into the genotypic differences within genotypes across their respective treatments (Supplementary Table S1). Unsurprisingly, highly significant genotypic differences were found for each genotype from GS 31 onwards ( $P < .001$ ). In contrast to the three commercial lines, Bibra BL was the only genotype that also recorded significant genotypic differences during the second measurement date ( $P < .001$ ). Furthermore, no significant genotypic differences were present before the commencement of the drought treatment (GS 26,  $P < .05$ ; Supplementary Table S1). The absence of variation at that specific time point accounts for their respective heritability. Furthermore, the results of the pairwise comparison are representative of what was found in Table 2 and Fig. 7.

In addition to genotypic differences within genotypes, the comparison also studied genotypic differences within treatment (Supplementary Table S2). Again, no significant differences were recorded for the first time point where treatment had not yet taken effect ( $P < .05$ ), confirming uniformity across all samples. Throughout the late tillering (GS29) and early stem elongation (GS31-32) stages, drought samples showed greater (significant) differences than well-watered samples. Conversely, the well-watered samples had more significant differences in the later growth stages, starting from late stem elongation (GS36) onwards (Supplementary Table S2).

The biplot derived from PCA summarised correlations between the different CT measurements at various growth stages for the drought, well-watered and field conditions (Fig. 8). To perform the PCA, three time-points were selected from the two experiments, namely late tillering (GS29), late stem elongation (GS25-36), and ear emergence (GS51-52). These time points were chosen based on overlapping growth stages once the flight dates of the UAV in the field were aligned with the thermal imaging dates of the lysimeter, along with the respective Zadoks' score of the plants at each date. The UAV data collected on the 26<sup>th</sup> of October 2022 has been excluded due to non-quality (negative  $H^2$ , data not shown). In the PCA, the well-watered condition of the lysimeter experiment is referred to as the optimal environment. As seen in Fig. 8, the first two PCs explained 79.4 % of the total variance in the data, with PC1 accounting for the majority (48%), followed by PC2 (31.4%). Almost all data points originating from the lysimeter experiment were negative for PC1 and all field data points were positive, suggesting that the variance in PC1 is driven by the two different experiments and their difference in conditions. The CT data recorded during Zadoks' growth stage 36 for the drought samples is however not negative for PC1. Additionally, this drought data point is most negatively correlated with the optimal- and field conditions ( $>90^\circ$  angle) while the optimal data points are positively correlated with the remaining drought conditions and some of the field conditions ( $<90^\circ$  angle). The biplot displays distinct patterns on PC2 where the effects of water stress are evident. Although most of the optimal and field groups are positive for PC2, all drought groups are negative. The environments in which more water was available appear to cluster together, with the exception of the field data around growth stage 51 where flowering stress is likely at cause. The PCA therefore confirmed the negative correlation between the lysimeter treatments as seen in Table 2 ( $P < .001$ ) and Fig. 7.

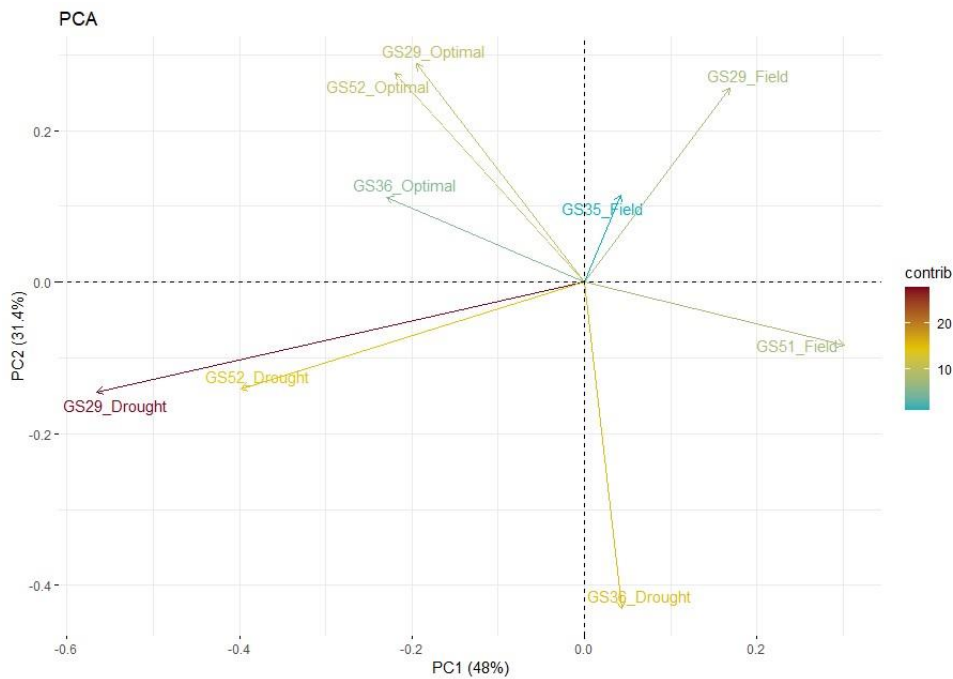


Figure 8: The relationships between the canopy temperatures of barley at three growth stages across three environments; drought, optimal (well-watered) and field (wet). The following growth stages were incorporated into PCA: late tillering (GS29), late stem-elongation (GS35-36) and ear emergence (GS51-52). The biplot displays results from principal component analysis (PCA), where principal component (PC) 1 and PC2 are shown and the contribution to the total variance per variable is indicated by their length and colour. The BLUPs from the spatial analysis were used for each data point.

### Barley Root Distribution under Wet Field Conditions

SpATS and HDM modelling revealed higher root counts at shallower depths than at deeper soil depths during the 2022 field trial (Fig. 9A). Additionally, the roots at deeper soil depths were less heritable (Fig. 9B). Furthermore, linear mixed models have detected that the core position and the run and range factors, as well as differences in root count operators, have a significant impact on the root count of each layer ( $P < .05$ ; Supplementary Table S3).

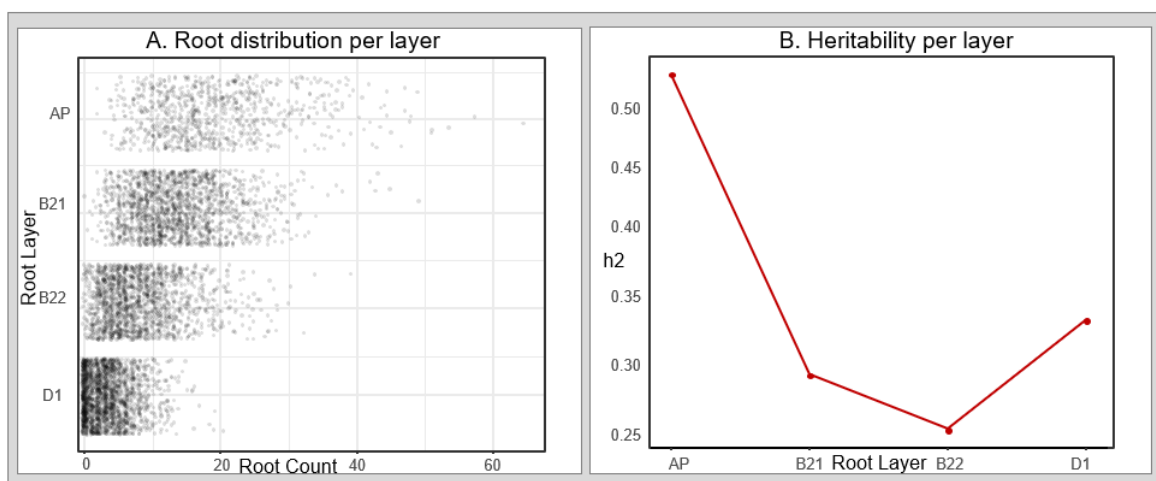


Figure 9: The root distribution (A) and heritability (B) of each layer of the combined root depths (AP, B21, B22, D1) for the 20 barley genotypes in the 2022 field trial conducted by the QAAFI research team.

### Relationships between Canopy Temperature and Rooting Depth

Through additional PCA, potential relationships between rooting depth and CT were explored. The resulting biplot showcases the four distinct root depth layers and the CT at one specific growth stage for each environment, represented as vectors (Fig. 10). The late stem-elongation growth stage (GS35/36) was selected based on the previously found adverse correlations between environments (Fig. 8). The two largest PCs captured 88.2% of the total variance between root- and CT traits (Fig. 10). PC1 accounts for 68.7% and separates the CT traits of the field and well-watered (optimal) conditions (positive for PC1) from the root traits and the CT traits of the drought condition (negative for PC1). This separation of the climate conditions based on water availability is similar to the one observed in PC2 of Fig. 8. In Fig. 10, the second PC accounts for 19.5% and segregates the field trial (positive for PC2) and the lysimeter experiment (negative for PC2) again. The PCA indicated a strong negative correlation ( $\sim 180^\circ$  angle) between CT traits in drought and the field conditions during the late stem-elongation stage in barley, which is explained by the extremely wet climate at the time of the field trial. Moreover, shallow root layers were negatively correlated with CT traits under optimal (well-watered) conditions. This indicates that increased roots in shallow root layers cause cooler CT under well-watered conditions. The limited amount of root growth in deeper layers during the field trial due to the wet climate is reflected in the PCA by the small contribution from B22 and D1. However, the deepest root layer (D1) is most associated with drought treatment as they share the same quadrant and track in similar directions (Fig. 10). The lack of substantial root growth in deeper soil layers prevents us from seeing accurate relationships between rooting depth and CT traits in drought.

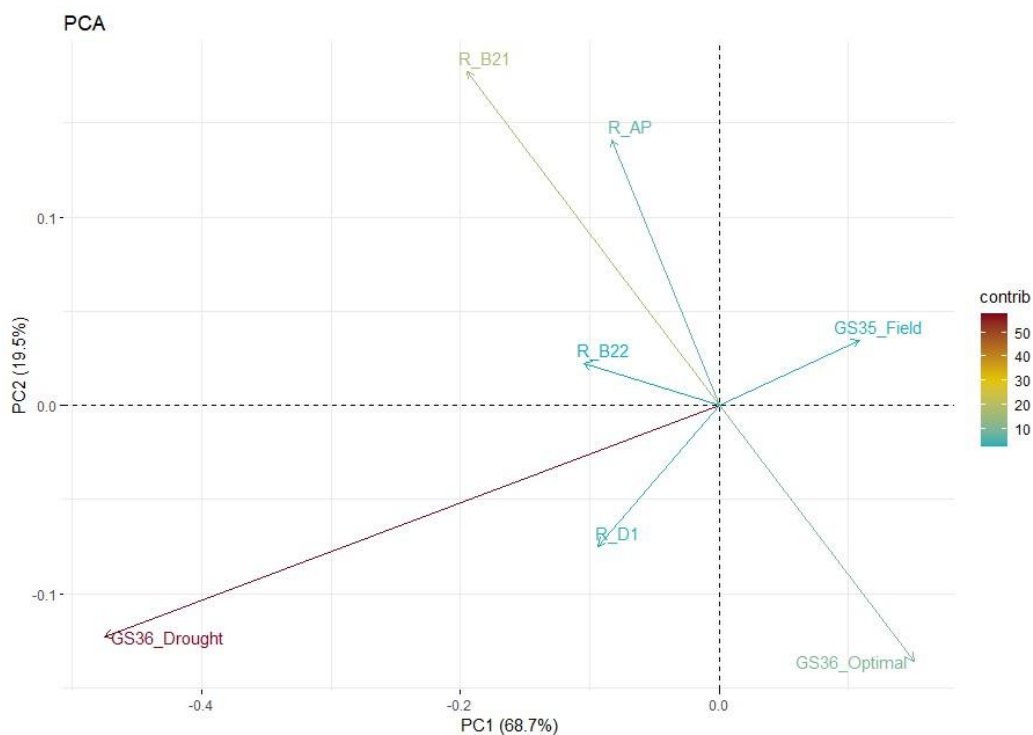


Figure 10: Biplot showing the principal component analysis (PCA) of rooting depth and the canopy temperature of barley at the late stem-elongation growth stage (GS35-36) across three environments; drought, optimal (well-watered) and field (wet). The rooting depths are clustered into four layers from the uppermost to the deepest layer: AP, B21, B22, and D1 (National Committee on Soil and Terrain & Isbell, 2016; Queensland Government, 2023). Principal component (PC) 1 and PC2 are displayed and the contribution to the total variance per variable is indicated by their length and colour. The BLUPs from spatial analysis were used for each data point.

### Changes in Other Above-Ground Traits

The rate of  $g_{sw}$  initially decreased dramatically upon implementation of drought, but increased for each genotype throughout August, with the highest levels recorded in September when the plants were close to flowering (Fig. 11). The changes of the  $g_{sw}$  characteristics exhibit a contrasting pattern when compared to that of CT, wherein an initial rise followed by a subsequent decline was observed (Fig. 7). The TC was only recorded until early stem-elongation (GS32), with a final count taken after harvest. Between the last two measurements, most genotypes showed a nearly triple increase in TC (Fig. 11). Notably, RGT planet had a much lower final TC compared to the other genotypes. Due to the lack of interim measurements between early stem elongation and flowering, it is unknown whether there was just an increase in TC during this phase, or if there was also a reduction in TC.

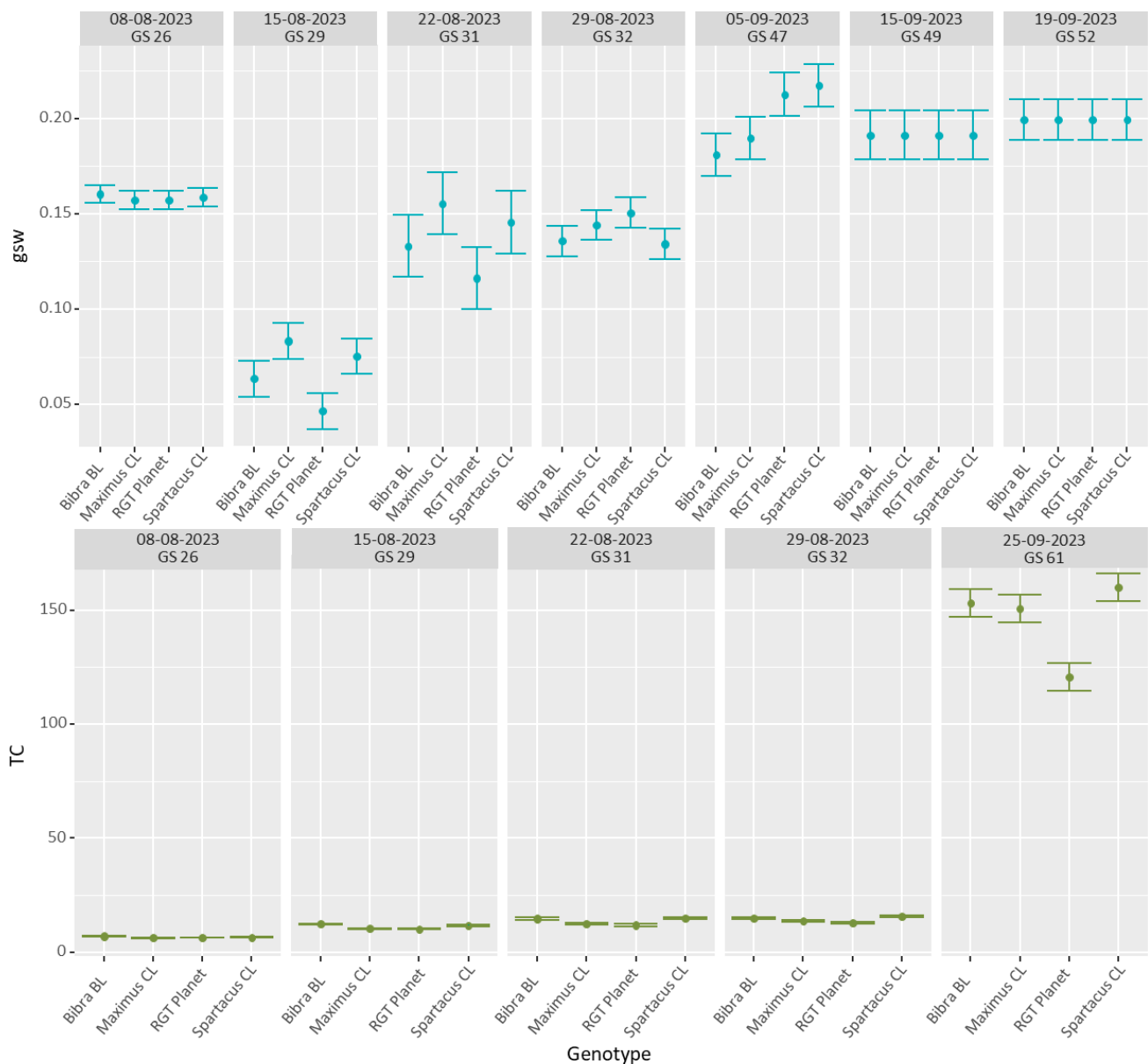


Figure 11: Spatially corrected stomatal conductance to water vapour ( $g_{sw}$ ) and tiller count (TC) for barley genotypes Bibra BL, Maximus CL, RGT Planet and Spartacus presented for each date/growth stage. Treatment has been accounted for as a fixed effect. The tiller count includes all tillers regardless of their reproductive status. Error bars reflect standard error.

Upon harvest, each tiller was classified as reproductive or non-reproductive (NR). This count showed that a greater proportion of tillers were NR during drought conditions as compared to well-watered conditions (Table 3).

Table 3: The mean percentage of non-reproductive (NR) tillers of the total tillers, for each genotype under drought- and well-watered treatments. Each value is based on eight replicates, except Maximus CL under drought treatment where there are only 7 replicates.

	% NR tillers in Drought	% NR tillers in Well-watered
Bibra BL	41.8	12.2
Maximus CL	34.6	10.6
RGT Planet	34.0	12.5
Spartacus CL	36.5	7.8

## Discussion

Although the negative impact of climate change on barley production is apparent, the direct effects on the RSA in barley are still largely unknown (Brown et al., 2019; ACCC, 2021). This is partly due to the limitations of traditional techniques used to study crop roots, which are often either time-consuming, laborious or inaccurate (Topp et al., 2016; McGrail et al., 2020). With hotter and drier weather becoming prevalent during the growing season, drought adaptation in barley is becoming increasingly urgent (WMO, 2023; Dijkman et al., 2017). Therefore, new rapid and indirect phenotyping tools are being evaluated to study the RSA of crops. Above-ground traits, especially canopy temperature (CT), offer such opportunities. Previous studies on crops like wheat and rice have suggested that cooler CT are linked to deeper root systems. Deeper root systems facilitate the plants with access to water. This allows for continued transpiration and in turn, leads to cooler canopies (Hirayama et al., 2006; Lopes & Reynolds, 2010; Pinto & Reynolds, 2015; Li et al., 2019).

In the current study, we used lysimeters to grow multiple barley genotypes in a controlled setting and under two climatic conditions: drought and well-watered. It was discovered that water availability affects the temperature of the canopy in barley as plants grown in a drought environment showed a significant increase in CT in comparison to the plants grown in an optimal, well-watered environment. However, the amount of variation in temperature between each treatment is different across the growth stages. The significant effects of treatment are abundant, by repeatedly appearing throughout various analyses in this study. This, in combination with the high heritability recorded during the lysimeter experiment, proves that the results of this experiment are reliable and highly repeatable. Drought stress was observed to be most intense during the stem-elongation stage, forcing drought-adaptive coping mechanisms to come into action in the lead-up to flowering, resulting in a drop in CT at later growth stages (Nakamichi, 2014; Trevaskis, 2018). This recovery in later growth stages is also confirmed by the positive correlation with earlier growth stages in which the drought stress was not prominent yet (Fig. 8). The increase in stomatal conductance during later growth stages suggests increased transpiration due to access to water, indicating that the plants under drought stress are undergoing adaptive changes and developing deeper roots to cope with the water stress. While drought conditions caused a reduction in productivity among the genotypes, significant genotypic differences in productivity under drought were unexplored during this research. However, genotypic differences were indicated by the final TC and these results would agree with the findings by Samarah et al. (2009), who reported genotypic and environmental differences in yield

across four barley genotypes that were exposed to well-watered, mild drought and severe drought treatments. Although it is not necessary, the increased number of NR tillers in drought-treated barley plants may indicate a decrease in yield under drought conditions, emphasizing the need for drought adaptation in barley.

Moreover, comparisons of the lysimeter results with the previously conducted field trial found negative correlations between CT in a drought and CT in an overly wet environment. During the wet field conditions, more shallow roots were grown. Due to the readily available amount of water, there was no need for the crop to grow deeper root systems. Shallow root systems in wet conditions have previously also been observed as a mechanism to prevent waterlogging in certain barley and wheat cultivars (Haque et al., 2012; Luan et al., 2023). These shallow layers of roots were negatively correlated with the CT of the plants in well-watered, optimal conditions during the lysimeter experiment. This study therefore demonstrated that barley cultivars with shallow root systems have cooler canopies in wet environments. Low heritability for deeper root layers demonstrates that roots in deeper soil layers are highly dependent on environmental factors. This indicates that the root results at deeper soil layers of this field experiment are likely to change depending on the climatic conditions. Currently, insufficient growth during the field trial at deeper layers hinders us from fully establishing the relationship between deeper roots and CT during drought conditions. Cooler canopies were expected to be associated with deeper roots under drought conditions in barley, and while the increase in  $g_{sw}$  and the drop in CT close to flowering suggests this deeper root growth development, further research is needed to confidently confirm our hypothesis. Root analysis of the root samples of the RRPAD lysimeter experiment may provide further insight into this relationship under drought stress. Although the results of the lysimeter experiment show high repeatability (>80% heritability upon commencement of climatic treatment), further research in the form of a field trial with drought conditions is necessary to fully explore the association of cooler CT and deeper RSA in barley under drought conditions. The results of the RPAD lysimeter experiment would not suffice alone due to the limitations in rooting depth, as the layer of soil in the lysimeter cores is only 70 cm deep. This may not capture deeper root growth accurately as roots were seen to collect at the bottom of the cores. In future research where rooting depth is of importance, a different lysimeter with deeper soil cores may be proven to be more beneficial.

## Conclusion

During this study, the usage of CT as a suitable phenotyping tool for barley roots and the relationship between CT and roots under drought conditions were investigated. It was demonstrated that CT varies across different climatic conditions and that significantly warmer CT were recorded during drought. We also observed changes in patterns in CT and other above-ground traits when flowering is near under drought conditions, due to the activation of the drought-adaptive coping mechanisms during later growth stages. Lastly, cooler canopies under well-watered conditions are found to be associated with shallow root systems and the increase in  $g_{sw}$  paired with the reduction in CT suggests that cooler canopies under drought conditions are associated with deeper root systems in barley.

Although further research is necessary to confirm this relationship under drought, CT through thermography has been proven to be a quick and effective phenotyping tool to determine the RSA of barley across multiple genotypes and climatic environments. A field experiment with drought conditions, paired with the lysimeter results of the current research will provide the necessary confirmative insights into the relationship between CT and rooting depth under drought. This study

highlights the advantageous application of CT for breeders in selecting barley cultivars that possess drought-adaptive traits such as deep root systems, which ultimately help maintain barley yields.

## References

- Agisoft LLC (2021). Agisoft Metashape. St. Petersburg, Russia. [www.agisoft.com](http://www.agisoft.com)
- Australian Competition and Consumer Commission. (2021). *Bulk grain ports monitoring report 2019–20*. Canberra, ACT: Australian Competition and Consumer Commission. Retrieved October 25, 2023, from: <https://www.accc.gov.au/about-us/publications/serial-publications/bulk-grain-ports-monitoring-reports/bulk-grain-ports-monitoring-report-2019-20>
- Basu, S., Ramegowda, V., Kumar, A., & Pereira, A. (2016). Plant adaptation to drought stress. *F1000Research*, 5, F1000 Faculty Rev-1554, doi: 10.12688/f1000research.7678.1
- Brown, A., Agbenyegah, B. K., Xia, C., Mornement, C. & Miller, M. (2019). Australian crop report December 2019. *Australian Bureau of Agricultural and Resource Economics and Sciences (ABARES)*, 192, Canberra, September. CC BY 4.0, doi: 10.25814/5de06ae055ba7
- Brien, C. (2023). asremlPlus: Augments 'ASReml-R' in Fitting Mixed Models and Packages Generally in Exploring Prediction Differences. R package version 4.3.55, <https://CRAN.R-project.org/package=asremlPlus>.
- Bureau of Meteorology. (2023). *Climate statistics for Australian locations*. Retrieved September 11, 2023, from: <http://www.bom.gov.au/climate/data/>
- Butler, D. G., Cullis, B. R., Gilmour, A. R., Gogel, B. J. & Thompson, R. *ASReml-R Reference Manual Version 4.2*. VSN International Ltd. [www.vsn.co.uk](http://www.vsn.co.uk)
- Das, S., Massey-Reed, S. R., Mahuika, J., Watson, J., Cordova, C., Otto, L., Zhao, Y., Chapman, S., George-Jaeggli, B., Jordan, D., Hammer, G. L. & Potgieter, A. B. (2022). A High-Throughput Phenotyping Pipeline for Rapid Evaluation of Morphological and Physiological Crop Traits Across Large Fields. *IGARSS 2022 - 2022 IEEE International Geoscience and Remote Sensing Symposium*, Kuala Lumpur, Malaysia, 2022, 7783-7786, doi: 10.1109/IGARSS46834.2022.9884530.
- Deery, D. M., Rebetzke, G. J., Jimenez-Berni, J. A., James, R. A., Condon, A. G., Bovill, W. D., Hutchinson, P., Scarrow, J., Davy, R., & Furbank, R. T. (2016). Methodology for High-Throughput Field Phenotyping of Canopy Temperature Using Airborne Thermography. *Frontiers in plant science*, 7, 1808, doi: 10.3389/fpls.2016.01808
- Department of Primary Industries and Regional Development. (2018, January 18). *Zadoks growth scale*. Government of Western Australia. Retrieved July 25, 2023, from: <https://agric.wa.gov.au/n/2102>
- Dijkman, T. J., Birkved, M., Saxe, H., Wenzel, H. & Hauschild, M. Z. (2017). Environmental impacts of barley cultivation under current and future climatic conditions. *Journal of Cleaner Production*, 2017, 140(2), 644-653, doi: 10.1016/j.jclepro.2016.05.154
- ESRI (2020). ArcGIS Desktop. Environmental Systems Research Institute, Redlands, CA. <http://www.esri.com/software/arcgis>
- FAO. (n.d.). Crops and livestock products. License: CC BY-NC-SA 3.0 IGO. Retrieved October 31, 2023, from: <https://www.fao.org/faostat/en/#data/QCL>
- Geoscience Australia. (n.d.). Geodetic Calculator. Australian Government. <https://geodesyapps.ga.gov.au/sunrise>

- Haque, M., E., Oyanagi, A. & Kawaguchi, K. (2012). Aerenchyma Formation in the Seminal Roots of Japanese Wheat Cultivars in Relation to Growth under Waterlogged Conditions. *Plant Production Science*, 15(3), 164-173, doi: 10.1626/ppls.15.164
- Hellal, F., Mansour, H., Abdel-Hady, M., El-Sayed, S., & Abdelly, C. (2019). Assessment water productivity of barley varieties under water stress by AquaCrop model. *AIMS Agriculture & Food*, 4(3).
- Hirayama, M., Wada, Y. & Nemoto, H. (2006). Estimation of drought tolerance based on leaf temperature in upland rice breeding. *Breeding Science*, 56 (1), 47–54, doi: 10.1270/jsbbs.56.47
- Högy, P., Poll, C., Marhan, S., Kandeler, E., & Fangmeier, A. (2013). Impacts of temperature increase and change in precipitation pattern on crop yield and yield quality of barley. *Food chemistry*, 136(3-4), 1470–1477, doi: 10.1016/j.foodchem.2012.09.056
- IPCC. (2023) *Climate Change 2023: Synthesis Report*. Contribution of Working Groups I, II and III to the Sixth Assessment Report of the Intergovernmental Panel on Climate Change [Core Writing Team, H. Lee and J. Romero (eds.)]. IPCC, Geneva, Switzerland, 35-115, doi: 10.59327/IPCC/AR6-9789291691647
- Islam, M. Z., Park, B.-J., Jeong, S.-Y., Kang, S.-W., Shin, B.-K., & Lee, Y.-T. (2022). Assessment of biochemical compounds and antioxidant enzyme activity in barley and wheatgrass under water-deficit condition. *Journal of the Science of Food and Agriculture*, 102(5), 1995–2002, doi: 10.1002/jsfa.11538
- Kassambara, A. & Mundt, F. (2020). factoextra: Extract and Visualize the Results of Multivariate Data Analyses. R package version 1.0.7. <https://CRAN.R-project.org/package=factoextra>.
- Lesmes-Vesga, R. A., Cano, L. M., Ritenour, M. A., Sarkhosh, A., Chaparro, J. X., & Rossi, L. (2022). Rhizoboxes as Rapid Tools for the Study of Root Systems of Prunus Seedlings. *Plants*, 11(16), 2081. MDPI AG, doi: 10.3390/plants11162081
- Li, A., Zhu, L., Xu, W., Liu, L., & Teng, G. (2022). Recent advances in methods for *in situ* root phenotyping. *PeerJ*, 10, e13638, doi: 10.7717/peerj.13638
- Li, X., Ingvorsen, C. H., Weiss, M., Rebetzke, G. J., Condon, A. G., James, R. A., & Richards, R. A. (2019). Deeper roots associated with cooler canopies, higher normalized difference vegetation index, and greater yield in three wheat populations grown on stored soil water. *Journal of experimental botany*, 70(18), 4963–4974, doi: 10.1093/jxb/erz232
- LI-COR. (2023). *Using the LI-600 Porometer/Fluorometer: Instruction manual*. LI-COR, Inc.
- Lo, T. H., Rudnick, D. R., Ge, Y., Heeren, D. M., Irmak, S., Barker, J. B., Qiao, X., & Shaver, T. M. (2018). Ground-based thermal sensing of field crops and its relevance to irrigation management. *NebGuide*, G2301.
- Lopes, M. S. & Reynolds, M. P. (2010). Partitioning of assimilates to deeper roots is associated with cooler canopies and increased yield under drought in wheat. *Functional Plant Biology* 37, 147-156, doi: 10.1071/FP09121
- Luan, H., Li, H., Li, Y., Chen, C., Li, S., Wang, Y., Yang, J., Xu, M., Shen, H., Qiao, H. & Wang, J. (2023). Transcriptome analysis of barley (*Hordeum vulgare* L.) under waterlogging stress, and overexpression of the *HvADH4* gene confers waterlogging tolerance in transgenic *Arabidopsis*. *BMC Plant Biol* 23, 62, doi: 10.1186/s12870-023-04081-6

- Mahmood, T., Khalid, S., Abdullah, M., Ahmed, Z., Shah, M. K. N., Ghafoor, A., & Du, X. (2019). Insights into Drought Stress Signaling in Plants and the Molecular Genetic Basis of Cotton Drought Tolerance. *Cells*, 9(1), 105, doi: 10.3390/cells9010105
- Malcheska, F., Ahmad, A., Batool, S., Müller, H. M., Ludwig-Müller, J., Kreuzwieser, J., Randewig, D., Hänsch, R., Mendel, R. R., Hell, R., Wirtz, M., Geiger, D., Ache, P., Hedrich, R., Herschbach, C., & Rennenberg, H. (2017). Drought-Enhanced Xylem Sap Sulfate Closes Stomata by Affecting ALMT12 and Guard Cell ABA Synthesis. *Plant physiology*, 174(2), 798–814, doi: 10.1104/pp.16.01784
- Manfreda, S., McCabe, M., Miller, P., Lucas, R., Pajuelo Madrigal, V., Mallinis, G., Ben Dor, E., Helman, D., Estes, L., Ciralo, G., Müllerová, J., Tauro, F., de Lima, M., de Lima, J., Maltese, A., Frances, F., Caylor, K., Kohv, M., Perks, M., ... Toth, B. (2018). On the Use of Unmanned Aerial Systems for Environmental Monitoring. *Remote Sensing*, 10(4), 641, doi: 10.3390/rs10040641
- McGrail, R., Van Sanford, D., & McNear, D. (2020). Trait-Based Root Phenotyping as a Necessary Tool for Crop Selection and Improvement. *Agronomy*, 10(9), 1328, doi: 10.3390/agronomy10091328
- Mohan, N., Jhandai, S., Bhadu, S., Sharma, L., Kaur, T., Saharan, V., & Pal, A. (2023). Acclimation response and management strategies to combat heat stress in wheat for sustainable agriculture: A state-of-the-art review. *Plant science: an international journal of experimental plant biology*, 336, 111834, doi: 10.1016/j.plantsci.2023.111834
- National Committee on Soil and Terrain & Isbell, R. (2016). The Australian Soil Classification. CSIRO Publishing, doi: 10.1071/9781486304646
- Nakamichi, N. (2014). Adaptation to the Local Environment by Modifications of the Photoperiod Response in Crops, *Plant and Cell Physiology*, 56, 594–604, doi: 10.1093/pcp/pcu181
- Nezar, H. S. (2005). Effects of drought stress on growth and yield of barley. *Agronomy for Sustainable Development*, 25 (1), 145-149, doi: 10.1051/agro:2004064
- Oyanagi, A. (1994). Gravitropic response growth angle and vertical distribution of roots of wheat (*Triticum aestivum* L.). *Plant Soil*, 165, 323–326, doi: 10.1007/BF00008076
- Pérez-Valencia, D. M., Rodríguez-Álvarez, M. X., Boer, M. P., Kronenberg, L., Hund, A., Cabrera-Bosquet, L., Millet, E. J. & van Eeuwijk, F. A. (2022). A two-stage approach for the spatio-temporal analysis of high-throughput phenotyping data. *Sci Rep* 12, 3177, doi: 10.1038/s41598-022-06935-9
- Pinto, R. S., & Reynolds, M. P. (2015). Common genetic basis for canopy temperature depression under heat and drought stress associated with optimized root distribution in bread wheat. *TAG. Theoretical and applied genetics. Theoretische und angewandte Genetik*, 128(4), 575–585, doi: 10.1007/s00122-015-2453-9
- Posit team (2023). RStudio: Integrated Development Environment for R. Post Software, PBC, Boston, MA. <http://www.posit.co/>
- Pradhan, A., Aher, L., Hegde, V., Jangid, K. K. & Rane, J. (2022). Cooler canopy leverages sorghum adaptation to drought and heat stress. *Sci Rep*, 12, 4603, doi: 10.1038/s41598-022-08590-6
- Queensland Government. (2023). Soil and Land Information, Site Listing Report: Project LOC Site 6104 Observation 1. “Queensland Globe”. Geoscientific information: Soils. Retrieved 6 September 2023.

- R Core Team (2021). R: A language and environment for statistical computing. R Foundation for Statistical Computing, Vienna, Austria. <https://www.R-project.org/>
- Rebetzke, G. J., Rattey, A. R., Farquhar, G. D., Richards, R. A., & Condon, A. T. G. (2012). Genomic regions for canopy temperature and their genetic association with stomatal conductance and grain yield in wheat. *Functional plant biology: FPB*, 40(1), 14–33, doi: 10.1071/FP12184
- Rejeb, A., Abdollahi, A., Rejeb, K. & Treiblmaier, H. (2022). Drones in agriculture: A review and bibliometric analysis. *Computers and Electronics in Agriculture*, 198, 107017, 0168-1699, doi: 10.1016/j.compag.2022.107017
- Samarah, N. H., Alqudah, A. M., Amayreh, J. A. & McAndrews, G. M. (2009). The Effect of Late-terminal Drought Stress on Yield Components of Four Barley Cultivars. *Agronomy & Crop Science*, doi:10.1111/j.1439-037X.2009.00387.x
- Takahashi, H., & Pradal, C. (2021). Root phenotyping: important and minimum information required for root modelling in crop plants. *Breeding science*, 71(1), 109–116, doi: 10.1270/jsbbs.20126
- Teledyne FLIR. (n.d.). How Do You Calibrate a Thermal Imaging Camera? Retrieved July 26, 2023, from: <https://www.flir.com.au/discover/professional-tools/how-do-you-calibrate-a-thermal-imaging-camera/>
- Topp, C. N., Bray, A. L., Ellis, N. A., & Liu, Z. (2016). How can we harness quantitative genetic variation in crop root systems for agricultural improvement? *Journal of integrative plant biology*, 58(3), 213–225, doi: 10.1111/jipb.12470
- Trachsel, S., Kaeppler, S. M., Brown, K. M., & Lynch, J. P. (2011). Shovelomics: high throughput phenotyping of maize (*Zea mays* L.) root architecture in the field. *Plant and soil*, 341, 75-87, doi: 10.1007/s11104-010-0623-8
- Trevaskis, B. (2018). Developmental Pathways Are Blueprints for Designing Successful Crops. *Frontiers in plant science*, 9, 745, doi: 10.3389/fpls.2018.00745
- Wasson, A.P., Rebetzke, G.J., Kirkegaard, J.A., Christopher, J., Richards, R.A. & Watt, M. (2014). Soil coring at multiple field environments can directly quantify variation in deep root traits to select wheat genotypes for breeding. *Journal of Experimental Botany*, 65(21), 6231-6249, doi: 10.1093/jxb/eru250
- Weaver, J. E., Jean, F. C., & Crist, J. W. (1922). *Development and activities of roots of crop plants: a study in crop ecology*, 316. Carnegie institution of Washington.
- Wickham, H. (2016). *ggplot2: Elegant Graphics for Data Analysis*. Springer-Verlag New York. ISBN 978-3-319-24277-4, <https://ggplot2.tidyverse.org>.
- World Meteorological Organization. (2023). *WMO Global Annual to Decadal Climate Update (Target years: 2023–2027)*. World Meteorological Organization. [https://library.wmo.int/doc\\_num.php?explnum\\_id=11629](https://library.wmo.int/doc_num.php?explnum_id=11629).
- Zadoks, J. C., Chang, T. T. & Konzak, C. F. (1974), A decimal code for the growth stages of cereals. *Weed Research*, 14: 415-421, doi: 10.1111/j.1365-3180.1974.tb01084.x

Zia, R., Nawaz, M. S., Siddique, M. J., Hakim, S. & Imran, A. (2021). Plant survival under drought stress: Implications, adaptive responses, and integrated rhizosphere management strategy for stress mitigation. *Microbiological Research*, 242, 0944-5013, doi: 10.1016/j.micres.2020.126626.

## Appendices

### Supplementary figures

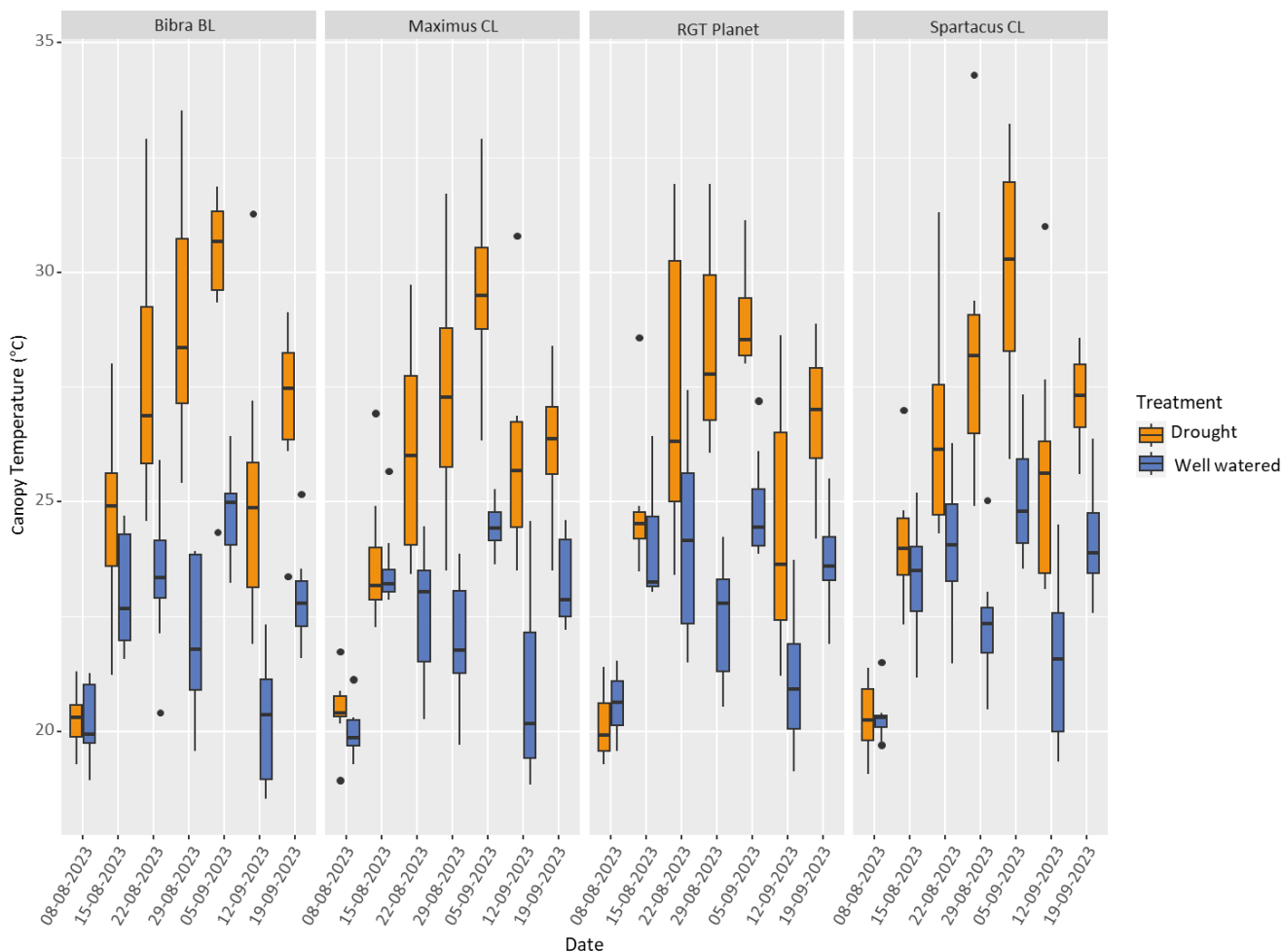


Figure S1: Recorded canopy temperatures (CT) for barley genotypes Bibra BL, Maximus CL, RGT Planet and Spartacus under drought- and well-watered treatments on seven dates. Black points present potential outliers.

### Supplementary tables

Table S1: Pairwise comparisons using Fisher's Least Significant Differences (LSD) for canopy temperature (CT) on seven dates within the genotypes Bibra BL, Maximus CL, RGT Planet and Spartacus CL between results under drought and well-watered treatment. Values are p-values and obtained based on Best Linear Unbiased Predictions (BLUPs). \*\*\* significant at  $p < 0.001$ , \*\* significant at  $p < 0.01$ , \* significant at  $p < 0.05$ . NS, not significant.

	Bibra BL		Maximus CL		RGT Planet		Spartacus CL	
<b>08-08-2023</b>	NS		NS		NS		NS	
<b>GS26</b>	0.175		0.100		0.763		0.633	
<b>15-08-2023</b>			NS		NS		NS	
<b>GS29</b>	0.000 ***		0.952		0.071		0.149	
<b>22-08-2023</b>								
<b>GS31</b>	0.000 ***		0.000 ***		0.000 ***		0.000 ***	

<b>29-08-2023</b>	<b>GS32</b>	0.000	***	0.000	***	0.000	***	0.000	***
<b>05-09-2023</b>	<b>GS36</b>	0.000	***	0.000	***	0.000	***	0.000	***
<b>12-09-2023</b>	<b>GS47</b>	0.000	***	0.000	***	0.000	***	0.000	***
<b>19-09-2023</b>	<b>GS52</b>	0.000	***	0.000	***	0.000	***	0.000	***

Table S2: Pairwise comparisons using Fisher’s Least Significant Differences (LSD) for canopy temperature (CT) on seven dates between the genotypes Bibra BL, Maximus CL, RGT Planet and Spartacus CL within their respective drought or well-watered treatment. Values are p-values and obtained based on Best Linear Unbiased Predictions (BLUPs). \*\*\* significant at  $p < 0.001$ , \*\* significant at  $p < 0.01$ , \* significant at  $p < 0.05$ . NS, not significant.

		Bibra BL	Maximus CL	RGT Planet	Spartacus CL
<b>08-08-2023 GS26</b>					
Bibra BL	Drought	NA	0.527 NS	0.457 NS	0.818 NS
Maximus CL	Drought		NA	0.167 NS	0.336 NS
RGT Planet	Drought			NA	0.610 NS
Spartacus CL	Drought				NA
Bibra BL	Well-watered	NA	0.788 NS	0.528 NS	0.356 NS
Maximus CL	Well-watered		NA	0.726 NS	0.518 NS
RGT Planet	Well-watered			NA	0.783 NS
Spartacus CL	Well-watered				NA
<b>15-08-2023 GS29</b>					
Bibra BL	Drought	NA	0.000 ***	0.988 NS	0.047 *
Maximus CL	Drought		NA	0.000 ***	0.030 *
RGT Planet	Drought			NA	0.030 *
Spartacus CL	Drought				NA
Bibra BL	Well-watered	NA	0.462 NS	0.009 **	0.308 NS
Maximus CL	Well-watered		NA	0.063 NS	0.763 NS
RGT Planet	Well-watered			NA	0.132 NS
Spartacus CL	Well-watered				NA
<b>22-08-2023 GS31</b>					
Bibra BL	Drought	NA	0.000 ***	0.640 NS	0.010 *
Maximus CL	Drought		NA	0.000 ***	0.132 NS
RGT Planet	Drought			NA	0.001 **
Spartacus CL	Drought				NA
Bibra BL	Well-watered	NA	0.157 NS	0.042 *	0.488 NS
Maximus CL	Well-watered		NA	0.002 **	0.048 *
RGT Planet	Well-watered			NA	0.221 NS
Spartacus CL	Well-watered				NA
<b>29-08-2023 GS32</b>					
Bibra BL	Drought	NA	0.000 ***	0.102 NS	0.312 NS
Maximus CL	Drought		NA	0.006 **	0.001 **

RGT Planet	Drought				NA		0.552	NS
Spartacus CL	Drought						NA	
Bibra BL	Well-watered	NA	0.705	NS	0.149	NS	0.414	NS
Maximus CL	Well-watered		NA		0.087	NS	0.256	NS
RGT Planet	Well-watered				NA		0.569	NS
Spartacus CL	Well-watered						NA	
<b>05-09-2023</b>		<b>GS36</b>						
Bibra BL	Drought	NA	0.312	NS	0.124	NS	0.989	NS
Maximus CL	Drought		NA		0.642	NS	0.293	NS
RGT Planet	Drought				NA		0.122	NS
Spartacus CL	Drought						NA	
Bibra BL	Well-watered	NA	0.697	NS	0.394	NS	0.205	NS
Maximus CL	Well-watered		NA		0.633	NS	0.094	NS
RGT Planet	Well-watered				NA		0.038	*
Spartacus CL	Well-watered						NA	
<b>12-09-2023</b>		<b>GS47</b>						
Bibra BL	Drought	NA	0.947	NS	0.319	NS	0.657	NS
Maximus CL	Drought		NA		0.306	NS	0.692	NS
RGT Planet	Drought				NA		0.136	NS
Spartacus CL	Drought						NA	
Bibra BL	Well-watered	NA	0.128	NS	0.049	*	0.001	**
Maximus CL	Well-watered		NA		0.629	NS	0.057	NS
RGT Planet	Well-watered				NA		0.176	NS
Spartacus CL	Well-watered						NA	
<b>19-09-2023</b>		<b>GS52</b>						
Bibra BL	Drought	NA	0.014	*	0.945	NS	0.493	NS
Maximus CL	Drought		NA		0.007	**	0.001	**
RGT Planet	Drought				NA		0.503	NS
Spartacus CL	Drought						NA	
Bibra BL	Well-watered	NA	0.260	NS	0.002	**	0.000	***
Maximus CL	Well-watered		NA		0.045	*	0.004	**
RGT Planet	Well-watered				NA		0.337	NS
Spartacus CL	Well-watered						NA	

Table S3: Linear mixed model results for root count in four different soil layers: AP, B21, B22 and D1. Run, range, operator and core position were tested for fixed effects. Values are p-values and obtained based on Best Linear Unbiased Predictions (BLUPs). \*\*\* significant at  $p < 0.001$ , \*\* significant at  $p < 0.01$ , \* significant at  $p < 0.05$ . NS, not significant.

Fixed effect	AP		B21		B22		D1	
Run	0.004	**	0.000	***	0.000	***	0.000	***
Range	0.000	***	0.000	***	0.000	***	0.000	***
Operator	0.000	***	0.000	***	0.002	**	0.075	NS
Core position	0.002	**	0.000	***	0.000	***	0.006	**

## Introduction

### System Overview

The RPAD Lysimeter is an automatic system that irrigates at three levels and provides periodic weighing to enable the calculation of water use on a half hour basis.

The system consists of 10 tables, each with 8 cores. A Phenolytics master controller communicates with the slave computer on each table. Firmware on the master controller allows the user to control when, at what level and how much water to apply to each core. The program records weights from each table at 30-minute intervals.

Data is stored in the master controller and is sent to a server to enable viewing in real time. In this way the system can be automatically monitored, and issues quickly identified.

### Operating platform

The RPAD master controller is operated online and can be accessed with any device, anywhere, anytime.

To provide data security, the RPAD Lysimeter uses two-factor authentication, a user assigned password and google authenticator random number generator.

The master controller is connected to our Phenolytics' server via any 4G provider. We recommend Telstra or Optus depending on the best signal from these two providers.

To access the 4G services, you will need to purchase and top up your data sim card.

It is advisable to contact your service technician to perform configuration changes or perform annual servicing tasks.

## Safety

### General Operation

**⚠ IMPORTANT:** Read and follow the instructions in the operation and maintenance manual before using the RPAD Lysimeter. Improper use can result in injury.

Allow only responsible adults who are familiar with the RPAD Lysimeter and its operation to use the RPAD Lysimeter.

Do not exceed the rated operating capacity.

Do not walk on the platform.

Always engage the foot brakes provided when parking or leaving the RPAD Lysimeters unattended.

Setup only in daylight or good artificial lighting.

Do not operate equipment while under the influence of alcohol or drugs, or while otherwise impaired.

Use caution when operating around 240VAC power cords. It is preferable to supply overhead power points to keep cords and plugs off the ground. If you see a damaged 240VAC power cord, turn off the RPAD mains power, tag out the site and immediately contact a licensed electrician.

**REMEMBER - Safety is your responsibility.**

# Specifications

<b>8 – Soil Cores</b>	
Pot dimensions	1000 x 300mm diameter
Water points	3 levels
<b>8 - Lysimeter scales</b>	
Type	Counter lever
Capacity	100kg
Safe service load	100%
Safe overload	150%
Ultimate overload	300%
Full load output	2mV/V $\pm$ 0.10%
Combined error	< 0.017%FS
Non-repeatability	< 0.01%FS
Creep/Zero return (30min)	< 0.02%FS
Zero balance	< 2.0%FS
Span temperature effect	< 15ppm/ $^{\circ}$ C
Zero temperature effect	< 26ppm/ $^{\circ}$ C
Compensated range	-10 $^{\circ}$ C to +40 $^{\circ}$ C
Operating range	-20 $^{\circ}$ C to +60 $^{\circ}$ C
Environmental protection rating	IP65
Material	Marine anodised aluminum
<b>1 – Onboard Controller</b>	
Inputs	<ul style="list-style-type: none"> <li>▪ Eight load cell ports – each with a regulated 12V DC power supply.</li> <li>▪ Two thermocouple inputs (type J or K).</li> <li>▪ A variety of modbus RTU compliant sensor modules such as soil temperature / moisture sensors, ambient air temperature / relative humidity sensors etc can be connected to the lysimeter module on any of its' eight modbus master ports.</li> </ul>
Outputs	<ul style="list-style-type: none"> <li>▪ Thirty-two solenoid driver outputs. These can be used for switching on and off relays, water solenoid valves etc.</li> <li>▪ Four 0-5V analog outputs can be used for controlling equipment such as precision peristaltic dosing pumps etc.</li> </ul>
Communication interface	<ul style="list-style-type: none"> <li>▪ Wi-Fi for networked communications with the I.T. system.</li> <li>▪ RS485 port for cable based read and control functions.</li> <li>▪ Modbus Master RTU RS485 port (RS485 type).</li> <li>▪ Proprietary communications interface for climate control. The lysimeter module is designed with this interface so that it can precisely control the temperature of an enclosed environment when interfaced to a specialised air conditioning unit.</li> </ul>

<b>1 - Data acquisition and upload</b>	
Local Network	Wifi
Data acquisition	Local storage
Remote access	Remote PC via 4G
<b>24 – Watering Valves</b>	
Operating voltage	12VAC
Operating pressure	10psi to 35psi
Material	316 Stainless steel
<b>1 – Master Valve</b>	
Operating voltage	12VAC
Operating pressure	10psi to 35psi
Material	316 Stainless steel
<b>4 – Castor Wheels</b>	
Size	Ø200mm
Load capacity	1000kg
<b>1 – Lysimeter Table</b>	
Material	316 Stainless Steel
Maximum combined load capacity	800kg
<b>Dimensions</b>	
W. Maximum Operating Width	1024mm
L. Maximum Operating Length	2360mm
H. Maximum Operating Height	1200mm
Lysimeter mass	200kg (approx.)

